ARTICLE

Engineering Low-Aspect Ratio Carbon Nanostructures: Nanocups, Nanorings, and Nanocontainers

Hyunkyung Chun,[¶,†] Myung Gwan Hahm,[¶,†] Yoshikazu Homma,[‡] Rebecca Meritz,[†] Koji Kuramochi,[‡] Latika Menon,[§] Lijie Ci,[⊥] Pulickel M. Ajayan,[⊥] and Yung Joon Jung[†,*]

[†]Department of Mechanical & Industrial Engineering, Northeastern University, Boston, Massachusetts, 02115, [‡]Department of Physics, Tokyo University of Science,Shinjuku, Tokyo 162-8601, Japan, [§]Department of Physics, Northeastern University, Boston, Massachusetts, 02115, and [⊥]Department of Mechanical Engineering & Materials Science, Rice University, Houston, Texas, 77005. [¶]These authors contributed equally to this work.

ABSTRACT The synthesis of carbon nanostructures, with interesting morphologies, has created a revolution in nanotechnology; carbon nanotube is a case in point, but other nanoscale morphologies of graphitic carbon could provide compelling uses. In particular short structures, including very short nanotubes, have proven impossible to be grown by existing techniques due to the difficulty in controlling and terminating growth during initial stages. Here we present architectures engineered from graphitic carbon, having up to 10^5 times smaller length/diameter (*L*/*D*) ratios compared to conventional nanotubes, revealing unique morphologies of nanocups, nanorings, and large area connected nanocup arrays. Such highly engineered hollow nanostructures were fabricated using precisely controlled short nanopores inside anodic aluminum oxide templates. The nanocups were effectively used to hold and contain other nanomaterials, for example, metal nanoparticles, leading to the formation of multicomponent hybrid nanostructures with unusual morphologies. The results reported here open up possibilities to integrate new morphologies of graphitic carbon in nanotechnology applications.

KEYWORDS: short carbon nanotubes · nanocups · nanorings · nanocontainer

Various groups have explored the potential of using unique hollow structures[1−6] from graphitic carbon, such as carbon nanotubes, for building multifunctional nanostructures[7−11] useful in a large number of applications.[12−17] However, current technologies are significantly limited by the difficulty of tailoring morphology and aspect ratio of individual nanoscale units.[18−21] Here, we demonstrate the design and fabrication of a new generation of hollow carbon nanostructures with unprecedented control in their length/diameter (*L*/*D*) aspect ratio, morphology, and dimension. We have been able to create, for the first time, morphologies which were challenging to make before, such as nanocups (*L*/*D* aspect ratio is 1−2), nanorings (*L*/*D* aspect ratio is less than 1 with open caps), and continuous films of connected nanocups. Our approach for fabricating these structures is shown schematically in Figure 1. For the synthesis of such highly engineered low aspect ratio carbon nanostructures, we developed a precisely controlled rational approach for creating extremely short nanochannels (channel diameter can be in the range of 30−100 nm) inside an anodized aluminum oxide (AAO) template, that has a 10^3-10^5 times smaller *L*/*D* aspect ratio compared to conventional AAO nanochannels. Once the template with designed short nanochannels is generated, we deposit the graphitic cup morphologies by the pyrolysis of acetylene at the temperature of 660 °C, without the use of any catalyst material. To make the graphitic nanoring morphology and to produce fully separated and length controlled nanocups, Ar ion milling was used. Also, we have used these unique nanocontainer geometries (cups) to contain and hold various metals of nanogram quantities. The templates can be removed by chemical etching to obtain isolated cups, rings, and connected arrays of these, having nanoscale dimensions.

RESULTS AND DISCUSSION

Figure 2 shows the scanning electron microscopy (SEM) and transmission electron microscopy (TEM) images of carbon nanocup arrays, connected with a continuous graphitic layer that holds them together. This film of connected nanocups produced by our method has three remarkable features in their structure and morphology. First, as shown in Figure 2a, a two-dimensional graphitic film with highly porous surface is achieved by connecting the highly dense and ordered arrays of nanocups together. Second, the resulting film of the nanocup arrays is flexible and remains intact even under strong physical deformation as shown in Figure 2b. Third,

*Address correspondence to jungy@coe.neu.edu.

Received for review February 24, 2009 and accepted April 21, 2009.

Published online May 1, 2009.
10.1021/nn9001903 CCC: $40.75

through the control of nanopore dimensions (diameter and length) we can precisely design and tailor the geometry and structure of the nanocups such as length, diameter, *L*/*D* aspect ratio, and their wall thickness. Figure 2c is a representative high magnification SEM image of a nanocup array, arranged in a highly ordered fashion with 100 nm diameter and 200 nm lengths. Shown in Figure 2d is the TEM image of arrays of connected nanocups (80 nm diameter and 80 nm length), clearly showing the formation of nanoscale cup geometry as well as a connected nanocup structure with 10 nm wall thicknesses. The image also indicates the flexibility of the two-dimensional nanocup array films with a polycrystalline and disordered graphitic structure of their lattice.

To synthesize individual nanocup and nanoring units with the full control over their *L*/*D* aspect ratio, Ar ion milling (300 V accelerating voltage and 55 mA emission current) was conducted on the connected arrays of nanocup film deposited in the AAO templates. A striking change in the structure and morphology of the nanocup films was observed during Ar ion irradiation as shown in Figure 3. After a few seconds (70 s) of Ar ion irradiation on the two-dimensional nanocup films, etching of a graphitic layer connecting the arrays of individual nanocups occurred and resulted in individually separated nanocup structures. Different lengths of nanocups could be obtained by controlling the ion milling time used for etching of the preformed nanocup films. Figure 3 panels a and b are SEM images of highly dense and completely separated nanocups with controlled *L*/*D* aspect ratio of 3 and 1, respectively. As the ion irradiation time increases beyond 70 s, the preferential etching of the bottom graphitic layer of carbon nanocups was initiated resulting in nanoscale tubular ring morphology. Figure 3 panels c and d are SEM images of multilayered and individually separated graphitic nanoring structures, respectively. The second layer of the nanoring arrays (Figure 3c) as well as the top surface of the supporting AAO templates (Figure 3d) could be observed through the nanoscale pores originating from the hollow ring morphology of nanorings formed by the Ar ion milling process. Detailed information on the morphological changes, from the connected nanocup films to the separated nanocup and nanoring structures, could be obtained by a TEM observation. Figure 3e shows side and top views of separated nanocups. It should be noted that graphitic carbon layers connecting individual nanocup structure were fully removed by the Ar ion-milling process. Also a high resolution TEM image (Figure 3f) of carbon nanorings indicates that the bottom layers of carbon nanocups were completely etched forming the ring geometry. It can be assumed that energetic Ar ions, traveling parallel to the short tubular axis of nanocups, preferentially etch the curved bottom layer of the nanocups by the Ar ion irradiation.

To elucidate the lattice structure and graphitization of the nanocup and nanoring structures, we have used

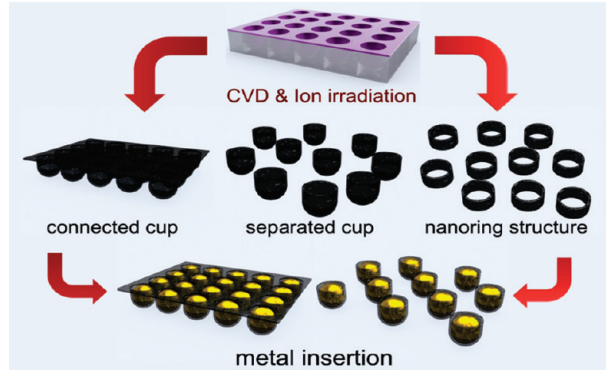

Figure 1. Schematic illustrating the fabrication process and resulting architectures of a connected arrays of nanocup film, individually separated nanocups, nanorings, and metal nanoparticle−nanocup heterostructures.

Raman spectroscopy with a 532 nm laser excitation in the spectral range of 1200−1700 cm^{-1}, in which we commonly observe the G band, ascribed to tangential modes of the graphene structure, and the disorder-induced D band, activated by the presence of defects.[22,23] Figure 4panels a and b show the result of Raman spectra observed from typical multiwalled carbon nanotubes (MWNTs), our nanocup, and nanoring structures of similar diameter. First, we have observed that the peak intensity ratio (I_D/I_G) has doubled as the structure changes from long MWNT (10 μm length) to extremely short nanoring structures (40 nm length). This result indicates a higher degree of disorder[24] in the nanoring structures

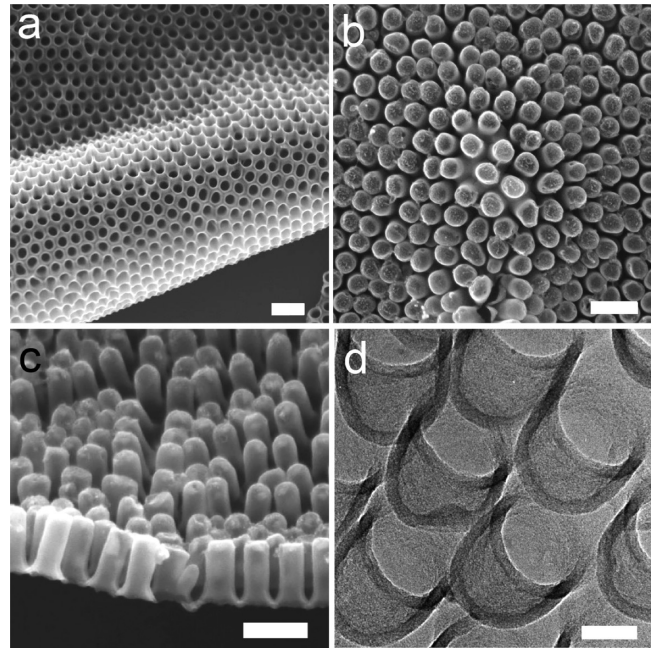

Figure 2. SEM and TEM micrographs of a two-dimensional carbon nanocup film structure after removing the AAO template. SEM images show (a) the bottom of highly dense carbon nanocup arrays connected with a thin graphite layer, (b) a two-dimensional and flexible film of carbon nanocups, and (c) the side view of carbon nanocups (100 nm diameter and 200 nm length) connected with a graphitic layer of 10 nm thicknesses. Scale bars are 200 nm. (d) A TEM image shows connected arrays of carbon nanocup film with 80 nm diameter and 80 nm length. A scale bar is 50 nm.

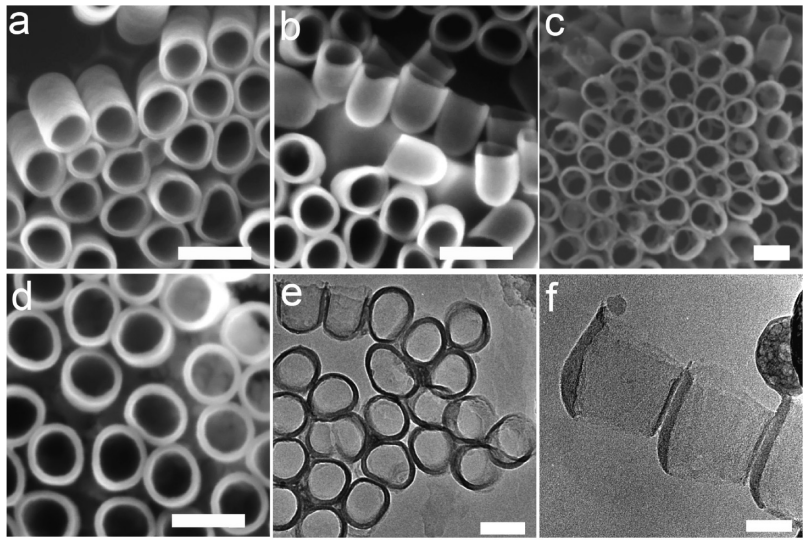

Figure 3. SEM images showing architectures of individual carbon nanocup and nanoring structures fabricated using an Ar ion milling process on the connected arrays of carbon nanocup film: (a) nanocups with the *L*/*D* aspect ratio of 3, (b) nanocups with the *L*/*D* aspect ratio of 1, (c) multilayered carbon nanoring arrays, and (d) single-layered nanoring arrays. Scale bars are 100 nm. TEM images from tailored carbon nanostructures clearly reveal nanoscale (e) cup and (f) ring morphology. Scale bars are 100 nm and 50 nm, respectively.

due to the Ar ion irradiation and lower *L*/*D* aspect ratio. The second noticeable change in Raman spectra is the blue-shift (upshift) of G band peak position (Figure 4a). For MWNT and carbon nanocup structures, the usual G band is observed around 1600 cm^{-1}.[24] However, G band spectra of nanorings with 60 and 40 nm lengths were recorded at 1607 and 1612 cm^{-1}, respectively. Such blue-shift of G band modes in the nanoring structures appears by D′ peak merges in the G band.[25] The D′ band is at ~1620 cm^{-1} and associated with the maximum in the 2D phonon density of states in graphene.[22,26] The mergence of G and D′ bands were obviously confirmed in full widths at half-maximum (FWHMs) of individual G band spectrum. The FWHMs of nanoring structures were slightly broadened from 28 to 44 wave numbers. The increase of I_D/I_G and the blue-shift of G band peak position might be caused by nanocrystallization of graphitic structure.[25] To understand these engineered graphitic nanostructure further, we also measured contact angle change of deionized water on continuous nanocup film before (Figure 4c) and after (Figure 4d) Ar ion milling process. As shown in Figure 4c, the contact angles of water droplet on the connected nanocup film are ranged from 69° to 73° indicating the hydrophobicity of nanocup structures. However, after Ar ion irradiation on the connected carbon nanocup film, the contact angles between surface of engineered graphitic nanostructures and deionized water droplet were dramatically reduced to 0° showing hydrophilic property as shown in Figure 4d. This might be due to the high density of disorders and nanocrystallized graphitic lattice formed from the Ar ion irradiation.[27]

The open nanoscale cup geometry as well as their graphitic nature make carbon nanocup structures a powerful template to act as container systems at the nanoscale. We have successfully inserted various metals inside the nanocups by using an e-beam evaporation followed by a thermal annealing process under an Ar environment. Figure 5 shows a collection of diverse carbon nanocup structures holding gold and lead inside. During the annealing process, the deposited metal inside the nanocups could be thermally re-evaporated into small metal nanoparticles seen inside the nanocups. As shown in Figure 5 panels c and d, we were also able to control the size of inserted metal nanoparticles by controlling the thickness of a metal film deposited. In SEM images, one can easily observe gold and lead nanoparticles inside the nanocups, as they are visible through the thin graphitic walls. TEM images show that gold nanoparticles are formed only within the pores of connected and isolated nanocups (Figure 5e,f) resulting in unique heteroarchitectures of carbon−metal materials.

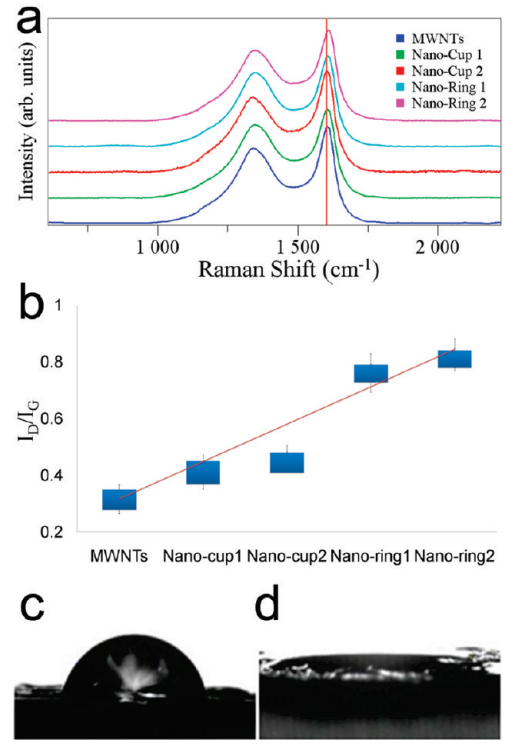

Figure 4. (a) Micro-Raman spectra (using 532 nm wavelength laser probe) taken from MWNTs (10 μm length), long nanocups (180 μm length), short nanocups (60 nm length), long nanorings (60 nm length), and short nanorings (40 nm length) (b) Histogram of the intensity ratio between the D band and G band (I_D/I_G) of each structure. I_D/I_G is increased from 0.34 to 0. 81 as the structures change from MWNTs to short nanorings. Optical images showing contact angle change of deionized water from (c) 72.38° to (d) 0° before and after Ar ion irradiation on connected carbon nanocup film.

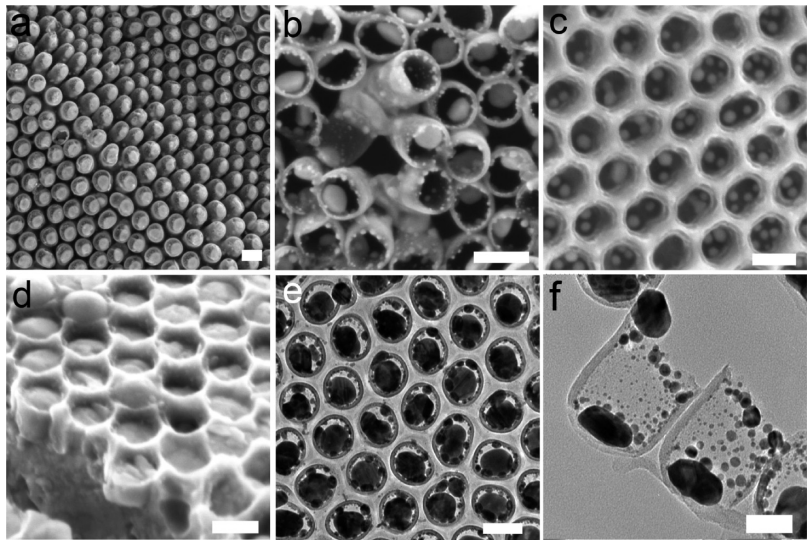

Figure 5. A collection of various carbon nanocup-based heterostructures. Ordered arrays of gold nanoparticles were formed selectively inside pores of both (a) carbon nanocup film structure and (b) individual nanocup and nanoring structures. The size of metal nanoparticles inside of nanocup structures can be controlled by adjusting the thickness of a deposited metal film. (c) Lead nanoparticles (10−15 nm diameters) formed directly from the lead film with 30 nm thickness during thermal annealing process. (d) A single lead nanoparticle (70−80 nm diameters) inserted from the lead film with 60 nm thickness during a thermal annealing process. TEM images of gold inserted (e) carbon nanocup films and (f) fully separated individual nanocups. All scale bars are 100 nm.

CONCLUSIONS

In conclusion, we demonstrate new graphitic architectures having extremely low L/D aspect ratio with unique nanoscale cup and ring geometries. Using these diverse nanoscale structures as templates, we can successfully insert various metals inside their pores to create multicomponent nanostructures and nanoscale container systems. The results reported here will allow us to build highly engineered and multicomponent functional nanobuilding blocks for various applications including nanomedicine (containers for nanogram quantities of materials, in drug delivery) and nanometrology (nanoscale unit measures).

EXPERIMENTAL METHODS

Preparation of Short Nanochannels inside of AAO Template. Nanoporous alumina template was prepared using a standard electrochemical anodization process described in detail elsewhere.[28,29] To produce highly ordered arrays of nanopores, a two-step anodization process was used. In the first step, a high purity Al foil (Alfa Aesar, 99.99%) was anodized at 40−45 V for 4 h in 3−5% oxalic acid ($C_2H_4O_2$) solution at room temperature. The anodized Al film was placed in the solution containing a mixture of 5% phosphoric (H_3PO_4) and 5% chromic (H_2CrO_4) acids for 24 h to remove the formed aluminum oxide layer. This process results in the formation of a well-ordered array of scallop-shapes on the aluminum surface.[30] A reanodization process was then performed but in precisely controlled and extremely short time (for 20−40 s) to fabricate highly organized short nanochannels (80−200 nm in length) giving 10^3-10^5 times smaller *L/D* aspect ratio. Then, samples were soaked in a 5% phosphoric acid solution for 1 h, which results in the widening of nanopores.

Deposition of Carbon Nanostructures inside AAO Template. Low aspect-ratio carbon nanostructures were synthesized by using a chemical vapor deposition (CVD) process.[31] The AAO template was first placed in a quartz tube and evacuated to 15 mTorr. During heat-up, high purity argon gas (99.9%) was supplied and the pressure was maintained at 760 Torr. When the temperature of the inside quartz tube reached 660 °C, acetylene (5 sccm)−argon (45 sccm) mixture gas was supplied as a carbon source for the deposition of a graphitic carbon layer inside predesigned short AAO nanochannels resulting in the connected arrays of carbon nanocup film structure.

Modification of Carbon Nanostructures. To fabricate separated and length controlled nanocup and nanoring structures, Ar ion-milling was used. We first load the connected carbon nanocup film inside of the ion milling chamber with a 90° incident angle and evacuated the chamber to 5×10^{-6} Torr. After that 35 sccm of argon is flowed into the system, creating a 2×10^{-4} Torr working pressure. Then 250 V beam voltage and the 55 mA beam current push electrons off the filament to ionize the argon atoms. We also set the accelerating voltage to 300 V to accelerate the argon cations. Ar ion-milling process was run for 70 and 120 s to fabricate and length-controlled separate nanocups and nanorings, respectively.

Fabrication of Highly Ordered Metal Nanoparticle−Nanocup Heterostructures. Gold with 80 nm thickness was deposited on the carbon nanocup structures (both connected arrays and individually separated ones) inside of the AAO template by using electron beam evaporation. Then gold-deposited carbon nanocup structures were annealed at 600 °C for 6 h under an Ar atmospheric environment. For lead, 60 nm thickness films were deposited on the carbon nanocup structures inside of the AAO template using a thermal evaporator, and then the template was annealed at 500 °C for 6 h under an Ar atmospheric environment. The size of metal nanoparticles inside of nanocup structures can be controlled by adjusting the thickness of a deposited metal film.

Template Removal. Carbon nanostructures inside of AAO were released by dissolving the AAO template in 33% hydrofluoric acid solution for as deposited nanocups as well as gold-inserted nanocup containers.

Acknowledgment. We are grateful for financial support from the NSF-NER program and the Center for High Rate Nanomanufacturing (NSF-NSEC) at Northeastern University. Y.J.J. acknowl-

edges support from a Provost Office Research Grant at Northeastern University and the technical advice on Raman analysis from Dr. Eunah Lee at Horiba Jobin Yvon Co. P.M.A. and L.C. acknowledge the focus center program for Interconnects.

REFERENCES AND NOTES

1. Iijima, S. Helical Microtubules of Graphitic Carbon. *Nature.* **1991**, *354*, 56–58.
2. Kroto, H. W.; Heath, J. R.; O'Brien, S. C.; Curl, R. F.; Smalley, R. E. C 60: Buckminsterfullerene. *Nature* **1985**, *318*, 162–163.
3. Iijima, S.; Ichihashi, T. Single-Shell Carbon Nanotubes of 1-nm Diameter. *Nature* **1993**, *363*, 603–605.
4. Iijima, S.; Yudasaka, M.; Yamada, R.; Bandow, S.; Suenaga, K.; Kokai, F.; Takahashi, K. Nano-aggregates of Single-Walled Graphitic Carbon Nanohorns. *Chem. Phys. Lett.* **1999**, *309*, 165–170.
5. Krishnan, A.; Dujardin, E.; Treacy, M. M. J.; Hugdahl, J.; Lynum, S.; Ebbesen, T. W. Graphitic Cones and the Nucleation of Curved Carbon Surfaces. *Nature* **1997**, *388*, 451–454.
6. Ugarte, D. Curling and Closure of Graphitic Networks under Electron-Beam Irradiation. *Nature* **1992**, *359*, 707–709.
7. Meng, G.; Jung, Y. J.; Cao, A.; Vajtai, R.; Ajayan, P. M. Controlled Fabrication of Hierarchically Branched Nanopores, Nanotubes, and Nanowires. *Proc. Natl. Acad. Sci. U.S.A.* **2005**, *102*, 7074–7078.
8. Martin, C. R. Nanomaterials: A Membrane-Based Synthetic Approach. *Science* **1994**, *266*, 1961–1966.
9. Davydov, D. N.; Sattari, P. A.; AlMawlawi, D.; Osika, A.; Haslett, T. L.; Moskovits, M. Field Emitters Based on Porous Aluminum Oxide Templates. *J. Appl. Phys.* **1999**, *86*, 3983–3987.
10. Sui, Y. C.; Cui, B. Z.; Marti'nez, L.; Perez, R.; Sellmyer, D. J. Pore Structure, Barrier Layer Topography and Matrix Alumina Structure of Porous Anodic Alumina Film. *Thin Solid Films* **2002**, *406*, 64–69.
11. Allen, B. L.; Kichambare, P. D.; Star, A. Synthesis, Characterization, and Manipulation of Nitrogen-Doped Carbon Nanotube Cups. *ACS Nano* **2008**, *2*, 1914–1920.
12. Weda, P.; Trzebicka, B.; Dworak, A.; Tsvetanov, C. B. Thermosensitive Nanospheres of Low-Density Core−An Approach to Hollow Nanoparticles. *Polymer* **2008**, *49*, 1467–1474.
13. Ye, X.; Gu, X.; Gong, X. G.; Shing, T. K. M.; Liu, Z. F. A Nanocontainer for the Storage of Hydrogen. *Carbon* **2007**, *45*, 315–320.
14. Bai, X. D.; Zhong, D.; Zhang, G. Y.; Ma, X. C.; Liu, S.; Wang, E. G.; Chen, Y.; Shaw, D. T. Hydrogen Storage in Carbon Nitride Nanobells. *Appl. Phys. Lett.* **2001**, *79*, 1552–1554.
15. Zhong, D. Y.; Zhang, G. Y.; Liu, S.; Wang, E. G.; Wang, Q.; Li, H.; Huang, X. J. Lithium Storage in Polymerized Carbon Nitride Nanobells. *Appl. Phys. Lett.* **2001**, *79*, 3500–3502.
16. Ma, X.; Wang, E.; Zhou, W.; Jefferson, D. A.; Chen, J.; Deng, S.; Xu, N.; Yuan, J. Polymerized Carbon Nanobells and their Field-Emission Properties. *Appl. Phys. Lett.* **1999**, *75*, 3105–3107.
17. Broz, P.; Driamov, S.; Ziegler, J.; Ben-Haim, N.; Marsch, S.; Meier, W.; Hunziker, P. Toward Intelligent Nanosize Bioreactors: A pH-Switchable, Channel-Equipped, Functional Polymer Nanocontainer. *Nano Lett* **2006**, *6*, 2349–2353.
18. Lu, K. L.; Lago, R. M.; Chen, Y. K.; Green, M. L. H.; Harris, P. J. F.; Tsang, S. C. Mechanical Damage of Carbon Nanotubes by Ultrasound. *Carbon* **1996**, *34*, 814–816.
19. Shelimov, K. B.; Esenaliev, R. O.; Rinzler, A. G.; Huffman, C. B.; Smalley, R. E. Purification of Single-wall Carbon Nanotubes by Ultrasonically Assisted Filtration. *Chem. Phys. Lett.* **1998**, *282*, 429–434.
20. Liu, J.; Rinzler, A. G.; Dai, H.; Hafner, J. H.; Bradley, R. K.; Boul, P. J.; Lu, A.; Iverson, T.; Shelimov, K.; Huffman, C. B. Fullerene Pipes. *Science* **1998**, *280*, 1253–1256.
21. Venema, L. C.; Wildöer, J. W. G.; Tuinstra, H.; Dekker, C.; Rinzler, A. G.; Smalley, R. E. Length Control of Individual Carbon Nanotubes by Nanostructuring with a Scanning Tunneling Microscope. *Appl. Phys. Lett.* **1997**, *71*, 2629–2631.
22. Dresselhaus, M. S.; Eklund, P. C. Phonons in Carbon Nanotubes. *Adv. Phys.* **2000**, *49*, 705–814.
23. Sato, K.; Saito, R.; Oyama, Y.; Jiang, J.; Cançado, L. G.; Pimenta, M. A.; Jorio, A.; Samsonidze, G. G.; Dresselhaus, G.; Dresselhaus, M. S. D-Band Raman Intensity of Graphitic Materials as a Function of Laser Energy and Crystallite Size. *Chem. Phys. Lett.* **2006**, *427*, 117–121.
24. Tan, P.; Zhang, S. L.; Yue, K. T. O.; Huang, F.; Shi, Z.; Zhou, X.; Gu, Z. Comparative Raman Study of Carbon Nanotubes Prepared by DC Arc Discharge and Catalytic Methods. *J. Raman Spectrosc.* **1997**, *28*, 369–372.
25. Ferrari, A. C.; Robertson, J. Interpretation of Raman Spectra of Disordered and Amorphous Carbon. *Phys. Rev. B* **2000**, *61*, 14095–14107.
26. Dresselhaus, M. S.; Dresselhaus, G.; Sugihara, K.; Spain, I. L.; Goldberg, H. A. *Graphite Fibers and Filaments*; Springer Series in Materials Science; Springer: New York, 1988; Vol. 5.
27. Schrader, M. E. Ultrahigh Vacuum Techniques in the Measurement of Contact Angles. IV. Water on Graphite (0001). *J. Phys. Chem.* **1975**, *79*, 2508–2515.
28. Masuda, H.; Fukuda, K. Ordered Metal Nanohole Arrays Made by a Two-Step Replication of Honeycomb Structures of Anodic Alumina. *Science.* **1995**, *268*, 1466–1468.
29. Masuda, H.; Yamada, H.; Satoh, M.; Asoh, H.; Nakao, M.; Tamamura, T. Highly Ordered Nanochannel-Array Architecture in Anodic Alumina. *Appl. Phys. Lett.* **1997**, *71*, 2770–2772.
30. Li, F.; Zhang, L.; Metzger, R. M. On the Growth of Highly Ordered Pores in Anodized Aluminum Oxide. *Chem. Mater.* **1998**, *10*, 2470–2480.
31. Kyotani, T.; Tsai, L. F.; Tomita, A. Preparation of Ultrafine Carbon Tubes in Nanochannels of an Anodic Aluminum Oxide Film. *Chem. Mater.* **1996**, *8*, 2109–2113.